

pss-Header will be provided by the publisher

Review copy – not for distribution

(pss-logo will be inserted here  
by the publisher)

# Well-arrayed ZnO nanostructures formed by multi-annealing processes at low temperature

Dapeng Wang<sup>1</sup>, Zeming Li<sup>1</sup>, Toshiyuki Kawaharamura<sup>2</sup>, Mamoru Furuta<sup>2</sup>, Tadashi Narusawa<sup>1</sup>, and Chaoyang Li<sup>1,2</sup>

<sup>1</sup> Department of Electronic and Photonic Systems Engineering, Kochi University of Technology, 185 Miyanokuchi, Tosayamada-cho, Kami city, 782-8502 Kochi, Japan

<sup>2</sup> Institute for Nanotechnology, Kochi University of Technology, 185 Miyanokuchi, Tosayamada-cho, Kami city, 782-8502 Kochi, Japan

Received, revised, accepted  
Published online

**Keywords** ZnO, nanostructures, multi-annealing process, radio frequency sputtering, photoluminescence

\* Corresponding author: li.chaoyang@kochi-tech.ac.jp, Phone: +81 887 57 2747, Fax: +81 887 57 2714

A novel process of multi-annealing was proposed for forming well-arrayed ZnO nanostructures on as-deposited ZnO thin films that were prepared on quartz glass using a radio frequency (rf) magnetron sputtering at low temperature. It was found that the formation and morphology of ZnO nanostructures were strongly dependent on the reducing gas annealing processes. Oxygen ambient annealing between two reducing annealing processes had the effect of introducing more oxygen into the ZnO thin film, as well as improving the crystallinity of

the ZnO nanostructures. An intense photoluminescence peak centered at 504 nm was observed in the well-arrayed ZnO nanostructures, due to the large amount of oxygen vacancies which existed on the larger surface area of ZnO nanostructures formed after the multi-annealing processes at a low temperature of 430 °C. These results show that multi-annealing processes are very effective in forming well-arrayed and controllable ZnO nanostructures.

Copyright line will be provided by the publisher

**1 Introduction** Zinc oxide (ZnO), a wide direct band gap semiconductor with large exciton binding energy (60 meV) at room temperature, is one of the most promising II-VI compound semiconductors for optoelectronic devices [1]. Among the various ZnO-related nanostructures, one dimensional ZnO nanostructures have received increasing attention due to their properties and their potential application for nanodevices [2, 3]. Currently ZnO nanostructures are grown using several methods [4-6]. Vayssieres et al. [4] found that ZnO could easily be processed as nanowires or nanorods on solid using the sol-gel method. Ronning et al. [5] have investigated *T*-ZnO nanorods with different sizes and differently shaped legs synthesized by evaporating Zn particles under controlled conditions. However, a technique for producing well-arrayed and controllable ZnO nanostructures is still needed. In our previous research [7], we succeeded in forming ZnO nanostructures using reducing annealing. In order to further control and produce well-arrayed ZnO nanostructures, we developed a novel low-temperature multi-annealing process, which combines a

reducing annealing process and oxygen annealing process. Multi-annealing processes were investigated for further understanding of the growth and luminescent mechanisms of ZnO nanostructures. This study may give significant impetus to produce well-arrayed ZnO nanostructures for future industrial applications.

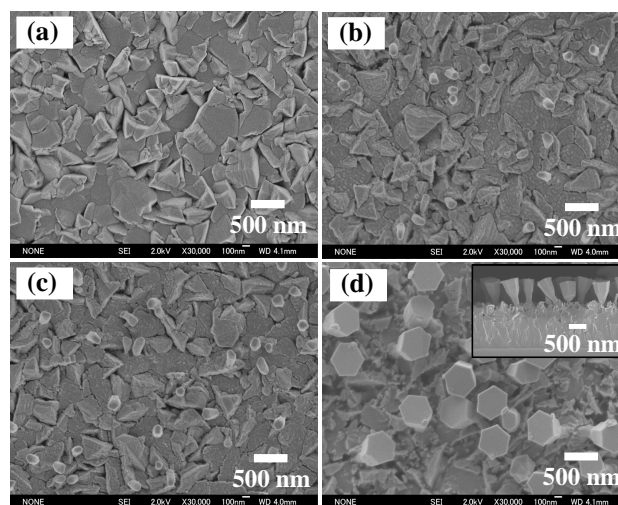
**2 Experimental** ZnO thin films (1 μm in thickness) were deposited on quartz glass by an RF (13.56 MHz) magnetron sputtering system using a sintered ZnO (5N) target. The substrate was heated and kept at 150 °C before and during deposition. Ar with a flow rate of 30 sccm was introduced into the chamber as the working gas. The deposition pressure was kept at 7 Pa with an RF power of 180 W. Following deposition, the deposited films were annealed at 430 °C in a conventional furnace in a series of steps: (I) forming gas (H<sub>2</sub> in N<sub>2</sub>: 2%) for 3 h, (II) oxygen for 1 h, (III) forming gas for 5 h. For safety, N<sub>2</sub> gas was introduced into the chamber for 5 min between step (I) and (II), and step (II) and (III).

Copyright line will be provided by the publisher

The crystal structure of the ZnO films was analyzed using an X-ray diffraction system (Rigaku ATX-G diffractometer), employing Cu K $\alpha$  ( $\lambda = 0.154178$  nm) radiation. The surface morphologies of the films were observed using a field emission scanning electron microscope (FE-SEM) system (JEOL-JSM7400F). The different luminescent characteristics of ZnO films under annealing process were measured by photoluminescence (PL) measurement, which was performed with an iHR320 Micro-PL/Raman spectroscope (Horiba Ltd.). A He-Cd laser with a wavelength of 325 nm at a power of 20 mW was used as an excitation light source. All of measurements were carried out at room temperature.

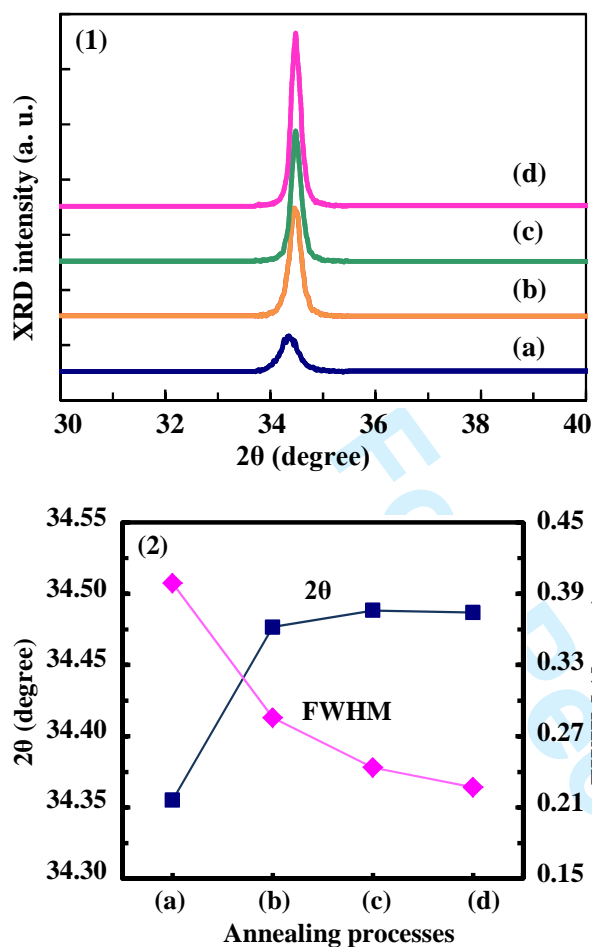
**3 Results and discussion** The morphologies of the as-deposited ZnO thin film and ZnO nanostructures were examined using an FE-SEM system, as shown in Fig. 1. It can be observed that the as-deposited ZnO thin film has a uniform and flat surface with an average grain size of about 300 nm. However, ZnO nanorods with uniform hexagonal heads have been vertically distributed on the ZnO films after annealing in the reducing ambient for 3 h. The evaluated diameter and height of nanorods are about 140 nm and 350 nm, respectively. After annealing in the oxygen ambient for 1 h, ZnO nanorods have grown slightly due to oxidation, without any change in the density of the nanostructures. The diameter and length of nanorods has increased to about 160 nm and 400 nm, respectively. Unexpectedly, higher density ZnO nanostructures of the reversed cones type with large hexagonal heads can be observed after annealing in the reducing ambient again for 5 h, as shown in the top view and cross-section of Fig. 1(d). The average diameter of the stems of formed ZnO nanostructures increases gradually from 160 nm at the bottom to 470 nm at the top. The average height of nanostructures is about 650 nm.

Figure 2(1) shows the XRD patterns of ZnO thin film and ZnO nanostructures obtained at each step of the multi-annealing processes. It is clear that the (002) diffraction peak is oriented highly perpendicular to the plane of the substrate for as-deposited ZnO film and nanostructures. Firstly, the (002) peak intensity of ZnO nanostructures is significantly increased after step I compared with as-deposited film, then substantially increases after step II and step III. Fig. 2(2) shows the position and the full width at half-maximum (FWHM) of the (002) diffraction peaks on post-treatment process. The peak position of as-deposited film shifts from  $34.35^\circ$  to a higher angle of  $34.47^\circ$ ,  $34.48^\circ$  and  $34.48^\circ$  after annealing step I, II and III, respectively. According to the (002) peak position of unstrained ZnO powder ( $2\theta = 34.42^\circ$ ), the compressive stress is confirmed to be released after annealing processes. The FWHM values of (002) diffraction peak sharply decrease from  $0.39^\circ$  of as-deposited film to  $0.28^\circ$ ,  $0.24^\circ$  and  $0.22^\circ$  after annealing step I, II and III, which indicates the crystallinity of the ZnO films is first significantly improved and then obviously enhanced with the post-treatment processes.



**Figure 1** SEM images of ZnO films (a) as-deposited and nanostructures obtained from annealed in (b) step I, (c) step I + II, and (d) step I + II + III. The inset SEM image is the cross section of ZnO nanostructures after the multi-annealing processes.

The growing mechanisms of formed well-arrayed ZnO nanostructures might include vapor-solid mechanism (VS) [8] and vapor-liquid-solid (VLS) mechanism [9], as described in our previous publication [7]. When the temperature increases, nuclear islands are quickly formed by the un-reacted zinc atoms on the surface of as-deposited thin film. Meanwhile, a reduction reaction, according to the reducing equation,  $H_2 + ZnO = Zn + H_2O$ , occurs on the surface of ZnO thin film when  $H_2$  is introduced to the furnace. With the temperature increased to over  $420^\circ C$  (the melting point of the zinc atom), the reduced Zn atoms would evaporate and adhere to the formed ZnO nuclei, serving as self-catalyst to form ZnO nanostructures along the preferential orientation path. During annealing in sufficient oxygen atmosphere (step II), Zn atoms produced from reduction reaction in step I would be oxidized to form ZnO, which contributes to slight regrowth of ZnO nanostructures as well as the introduction of oxygen into the ZnO thin film. Consequently, the crystallinity of nanostructures on thin films is significantly improved. During annealing again in reducing gas (step III), the growth mechanism is similar to that in step I. However, oxygen annealing in step II might increase the amount of oxygen in the surface of thin film and nanostructures. Therefore, the ZnO nanostructures could be regrown quickly in prioritized c-axis direction. When the reducing annealing time is further increased, the reduction product, i. e. formed  $H_2O$  vapor, will be increased as well. This vapor would be absorbed on the top of the ZnO nanorods, and suppress the  $H_2$  reducing effect on the top of ZnO nanorods. Consequently, the lateral growth of ZnO nanostructures will be enhanced. Finally, the ZnO nanostructures appeared as fluted reverse cones with hexagonal heads.



**Figure 2** (1) XRD patterns, (2) variation of peak position and the FWHM values obtained from ZnO films (a) as-deposited and annealed in (b) step I, (c) step I + II, and (d) step I + II + III.

Figure 3 shows the PL spectra of as-deposited ZnO thin film and ZnO nanostructures. It is difficult to find visible range emission in as-deposited ZnO thin film. The intensity of UV peak increases at each post-treatment step, which indicates that optical crystallinity is significantly improved. A broad green PL peak is obtained from the ZnO nanostructures after step I, which means that the oxygen vacancies are introduced by the reducing atmosphere annealing. This corresponds with the well-accepted green emission principle in ZnO thin film [10]. It is reasonable to assume that, due to the oxidation reaction, there is a remarkable yellow shift with degraded intensity of visible light emission after step II. This shift leads to a quantity of oxygen vacancies being partially neutralized in both the formed nanostructures and thin film during annealing in pure oxygen ambient. Furthermore, the much enhanced PL peak shifts back to 504 nm after annealing step III. According to the morphology of ZnO nanostructures that have bigger size hexagonal heads and greater height, it is possible to assume that many more oxygen vacancies are

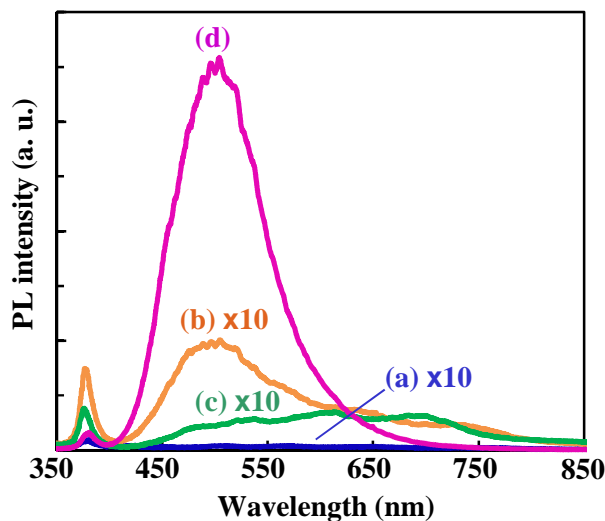


**Figure 3** PL spectra of ZnO films (a) as-deposited and annealed in (b) step I, (c) step I + II, and (d) step I + II + III, measured with the excitation power of 1 mW at room temperature.

produced by the lengthier annealing time and are present in the nanostructures with a larger surface area.

**4 Conclusion** The effects of multi-annealing processes on forming ZnO nanostructures on the ZnO thin films were investigated. Well-arrayed ZnO nanostructures with the appearance of fluted reverse cones capped with hexagonal heads were obtained via a novel multi-annealing process. The crystallinity of ZnO nanostructures was also improved. ZnO nanorods with oxygen vacancies contribute to green luminance after treatment in reducing gas. Oxygen annealing between the two reducing gas annealing processes contributed to efficiently introduce the oxygen into the ZnO thin films, leading to ZnO nanostructures regrown quickly. An intense green emission centered at 504 nm was obtained, ascribable to the large amount of oxygen vacancies on the formed enlarged surface of ZnO nanostructures after multi-annealing processes at a low temperature of 430 °C. Therefore, the multi-annealing process is an efficient method to form well-arrayed ZnO nanostructures, which might be applied in optoelectronic devices in the future.

**Acknowledgements** The authors gratefully acknowledge the support by Iketani Science and Technology Foundation.

## References

- [1] T. Soki, Y. Hatanaka, and D. C. Look, *Appl. Phys. Lett.* **76**, 3257 (2000).
- [2] M. H. Huang, S. Mao, H. Feick, H. Yan, Y. Wu, H. Kind, E. Weber, R. Russo, and P. Yang, *Science* **292**, 1897 (2001).
- [3] S. W. Lee, H. D. Cho, G. Panin, and T. W. Kang, *Appl. Phys. Lett.* **98**, 093110 (2011).
- [4] L. Vayssieres, *Adv. Mater.* **15**, 464 (2003).
- [5] C. Ronning, N. G. Shang, I. Gerhards, H. Hofsass, M. Seibt, *J. Appl. Phys.* **98**, 034307 (2005).

- 1  
2  
3  
4  
5  
6 1 [6] A. C. Mofor, A. S. Bakin, A. Elshaer, D. Fuhrmann, F.  
7 2 Bertram, A. Hangleiter, J. Christen, and A. Waag, *Phys. Stat.*  
8 3 *Sol. (C)* **3**, 1046 (2006).  
9 4 [7] C. Li, T. Kawaharamura, T. Matsuda, H. Furuta, T.  
10 5 Hiramatsu, M. Furuta, and T. Hirao, *Appl. Phys. Express* **2**,  
11 6 091601 (2009).  
12 7 [8] Z. Zhang, S. J. Wang, T. Yu, and T. Wu, *J. Phys. Chem. C*  
13 8 **111**, 17500 (2007).  
14 9 [9] P. X. Gao and Z. L. Wang, *J. Phys. Chem. B* **108**, 7534  
15 10 (2004).  
16 11 [10] M. Willander, O. Nur, J. R. Sadaf, M. I. Qadir, S. Zaman, A.  
17 12 Zainelabdin, N. Bano, and I. Hussain, *Materials* **3**, 2643  
18 13 (2010).  
19 14  
20 15  
21 16  
22 17  
23 18  
24 19  
25 20  
26 21  
27 22  
28 23  
29 24  
30 25  
31 26  
32 27  
33 28  
34 29  
35 30  
36 31  
37 32  
38 33  
39 34  
40 35  
41 36  
42 37  
43 38  
44 39  
45 40  
46 41  
47 42  
48 43  
49 44  
50 45  
51 46  
52 47  
53 48  
54 49  
55 50  
56 51  
57 52  
58 53  
59 54  
60 55  
57